

# Particle Swarm Optimisation-Based Support Vector Regression Model to Estimate the Powder Factor of Explosives in Groundwater Tunnel Driving



E. de Miguel-García, K. Martín-Chinea, and J. F. Gómez-González

**Abstract** In many parts of the world, especially in arid or semi-arid areas, they find drinking water in the subsoil. One way to reach it, it is through small horizontal tunnels (Qanat) built on the mountain using explosives. Civil engineers must design projects where they estimate the budget necessary to undertake the work, taking into account the amount of explosives needed, number of blasts, duration of the civil work and powder factor among other data. However, there is not artificial intelligence-based models that help to forecast the amount of explosive needed to drill a tunnel. In this work, a hybrid regression model based on support vector machine (SVM) and particle swarm optimization (PSO) trained with real data (types of lithologies, geomechanical characteristics of the rocks and the amount of explosives used by engineers based on their previous experiences) obtained from a volcanic groundwater tunnel driving in the island of Tenerife (Spain), is proposed to predict the advance, the amount of explosives, the number of blasts and the powder factor in new tunnels or expansion of existing ones. The results show that a new, simpler regression model has been obtained that reproduces the experimental data and it will reduce the effort of the engineers in the study of a new tunnel driving work.

**Keywords** SVM · PSO · Tunnel · Blast · Powder factor · Lithology

---

E. de Miguel-García (✉)  
Department of Agrarian, Nautical, Civil and Maritime Engineering,  
University of La Laguna, 38071 La Laguna, Tenerife, Spain  
e-mail: [emiguelg@ull.edu.es](mailto:emiguelg@ull.edu.es)

K. Martín-Chinea · J. F. Gómez-González  
Department of Industrial Engineering, University of La Laguna,  
38071 La Laguna, Tenerife, Spain  
e-mail: [kmartinc@ull.edu.es](mailto:kmartinc@ull.edu.es)

J. F. Gómez-González  
e-mail: [jfcgomez@ull.edu.es](mailto:jfcgomez@ull.edu.es)

## 1 Introduction

A large part of the fresh water used is underground water and horizontal tunnels or wells are used to reach it [1]. These tunnels have their origin in the Qanat of the Middle East that goes back to the 8th century BC [1]. Nowadays, it is a common practice to use explosives to drive groundwater tunnels for what is necessary a civil engineering study that will define the drilling and blasting designs will be used, schedule the civil work and forecast the budget necessary.

The forecast of amount of explosive used in the blast and the powder factor (ratio between the kilograms of explosive used and the volume of extracted material) is important to determinate the duration and the budget of the civil work. Drilling and blasting designs (D&B) for small-section tunnels have been defined to parallel hole-cuts by other authors [2–4] where the geomechanical characteristics of the rocks are taken into account.

In this field, there have not been really new advances related with the develop of computational tools that help the engineer to forecast better the amount of explosive needed to drill a tunnel, according to the expected lithology along the tunnel and the D&B used. In general, the no-linear relations between the different variables (geomechanical properties of the lithology, powder factor, D&B, etc.) and the limited number of experimental measurements make difficult to find a simple mathematical relationship [5].

The aim of the present work is to combine of the Support Vector Regression (SVR) [6–9] with Particle Swarm Optimization (PSO) [10, 11] to find a non-linear regression among the rock parameters, the number of blasts and powder factors to drive a tunnel. SVR is a machine learning based on the theory of statistical learning used in different fields of science and engineering to have predictions in complex problems [7, 12–16]. To optimize the parameters of the SVR the algorithm PSO is applied. PSO is a metaheuristic algorithm that was developed based on social systems of the swarm theory inspired by the movement of flocks of birds [12]. Therefore, this hybrid PSO-SVR model helps the civil engineer to predict the duration of the driving and to estimate the human and material resources necessary to execute it. In this study, this methodology is applied to a groundwater tunnel in the island of Tenerife, Spain.

## 2 Materials and Methods

### 2.1 Characterization and Measurement of Lithological Data

Data used in the present work were recorded on a real civil work in an underground water tunnel in the island of Tenerife, located in the Canary Islands (Spain), in the North East Atlantic Ocean off the coast of Africa. The civil work aims to 85.75 m plus a tunnel already built of 4000 m in length by blasting using a gelatin-based explosive

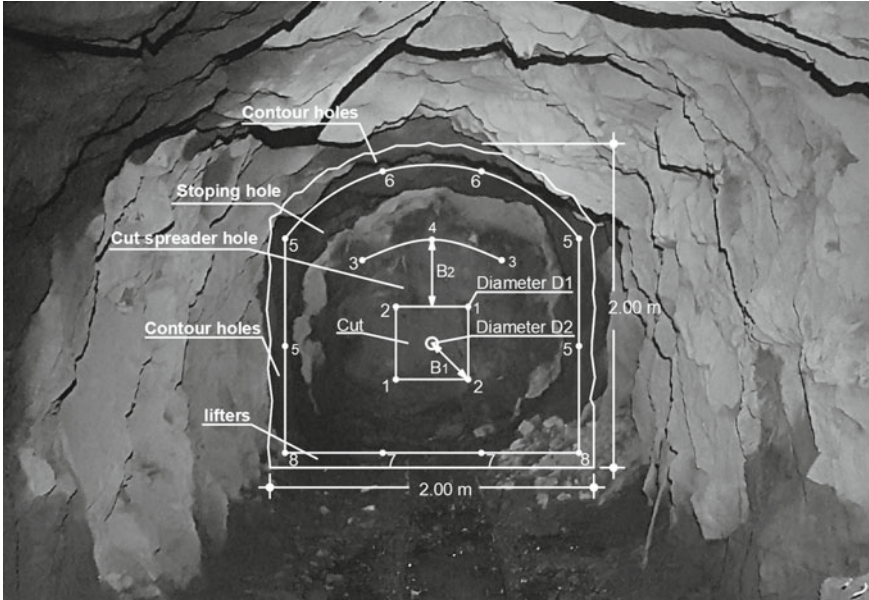


**Fig. 1** Geometric drill pattern. **a** Example of a blast pattern with 17 boreholes used in the tunnel of the present work based on the blasting manual, Geological and Mining Institute of Spain. This photography is the front of a tunnel after a blast

for civil and mining purposes (RIODINTM, MAXAM Europe, S.A. Madrid, Spain). This explosive is selected because the impedance of the rock (the impedance of the rock is the product of its density by the propagation velocity of the wave [17]) is similar to the impedance of the explosive to have an optimal fragmentation [18].

The drilling and blasting designs followed the specifications described by Langefors and Kihlstrom [2], commonly applied to these hydraulic works in tunnels on the island of Tenerife. The charge calculation for tunnel blasting, when the cross section is small, is defined by the 'cut', 'cut spreader hole', 'contour hole' and the 'lifters' for a cut of four sections with parallel holes (Fig. 1). The drill plan and the charging and firing pattern are based on the spacing between boreholes as well as the linear load per borehole, taking into account the characteristics of the lithology. In the case described here, the tunnel technicians used three drilling and blasting designs for the tunnel with 14, 16 or 17 blast-holes depending on the type of rock [19].

The mean average advance is limited in this design by the deviation of the loaded boreholes. Given this deviation is below 2%, the estimated advance is 95% of the length of the boreholes [20]. Typically, the water tunnels in the island of Tenerife are perforations in straight line with a gradient of 2% and a section of about 3.94 m<sup>2</sup> with a tunnel height of 2.00 m, a side wall height of 1.80 m, a rise of the arch 0.20 m and a width of 2.00 m. The tunnels cross a wide variety of volcanic rocks as it was described in [5].

The amount of the explosive used, the advance and an undisturbed rock with suitable dimensions (larger than 40 cm) were recorded from each blast. The rocks were tested in a licensed laboratory (Laboratories and Quality of Construction of the Ministry of Public Works and Transport, Vice-Ministry of Infrastructure and Transport of the Government of the Canary Islands, Spain) to determinate their geological and geotechnical properties.

Samples ( $n = 48$ ) were identified with eight different lithotypes (Fig. 2a): (a) aphanitic massive basalt, (b) altered and highly altered aphanitic massive basalt, (c) vacuolar aphanitic basalt (vacuole  $<0.05$  mm), (d) vacuolar aphanitic basalt (vacuole  $<0.3$  mm), (e) phonolite, (f) red colour ignimbrite, (g) highly altered red colour ignimbrite (vacuolar basaltic fragments), (h) agglomerate basaltic materials [21]. In order to characterize the eight lithotypes found, the following averaged parameters were calculated: point load strength index  $I_s$  (MPa), density ( $\text{g}/\text{cm}^3$ ) and open porosity  $P$  (%). To compare the values, data were normalized by the averaged maximum found in the eight lithologies (Fig. 2a). In addition, the Fig. 2b shows the averaged quantity of explosive and pull (advance) and the powder factor for each lithotypes.

## 2.2 Support Vector Regression

The support vector machine (SVM) [7, 22] for regression (SVR) is used to forecast the advance (pull) when it is known the geomechanical properties of the lithology and the kilograms of explosive needed to excavate a tunnel. SVR tries to found the hyperplane that is near as many data as possible minimizing the sum of the distances from the data points to the hyperplane based on statistical learning theory [16]. When the error  $\varepsilon$  between the predicted and the real values is assumed based on the experience, the used method is named the  $\varepsilon$ -SVR. In this article, the  $\nu$ -support vector regression ( $\nu$ -SVR) [23–25] a modification of  $\varepsilon$ -SVR [8] is used, where the parameter  $\nu \in (0,1]$  controls the number of support vectors and the training errors [6, 25] minimising the error  $\varepsilon$  automatically. The SVR is implemented using the library LIBSVM [26].

The optimization problem of  $\nu$ -SVR is defined as follows.

$$\min_{w,b,\xi,\xi^*,\varepsilon} \left\{ \frac{1}{2} \| \mathbf{w} \|^2 + C \left( \nu \varepsilon + \frac{1}{l} \sum_{i=1}^l (\xi_i + \xi_i^*) \right) \right\} \quad (1)$$

$$(\mathbf{w}^T \phi(\mathbf{x}_i) + b) - y_i \leq \varepsilon + \xi_i$$

$$y_i - (\mathbf{w}^T \phi(\mathbf{x}_i) + b) \leq \varepsilon + \xi_i^*$$

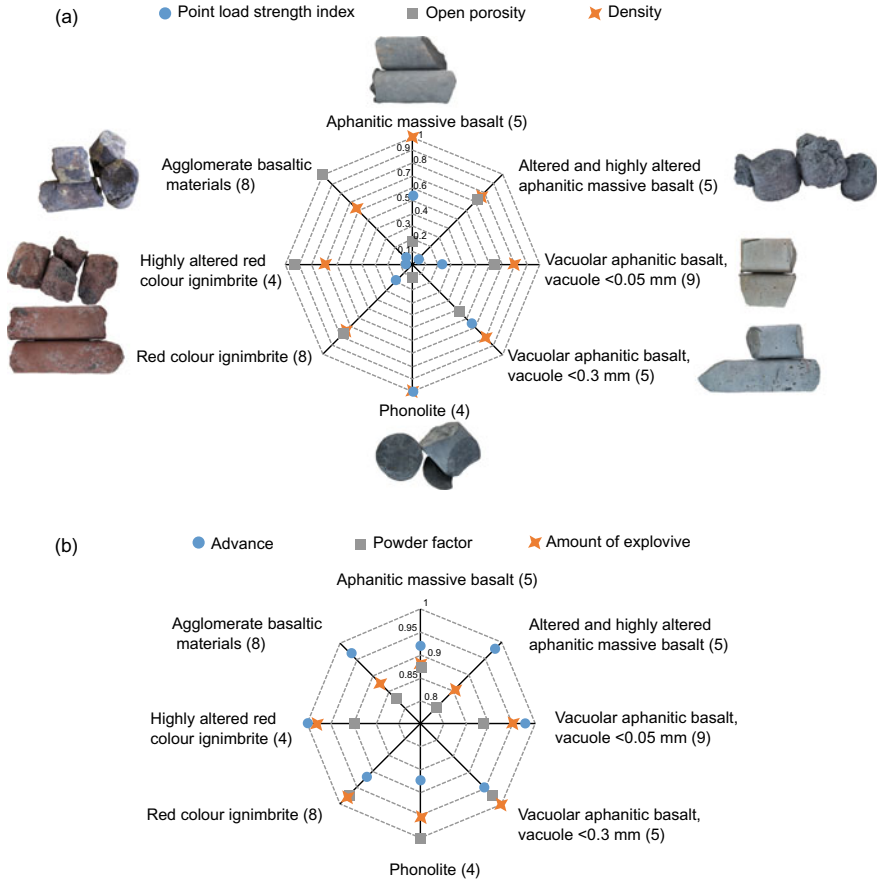


**Fig. 2** Characteristic parameters for each lithotype and blasting information. Values are normalized by maximum averaged value for each parameter: point load strength index 5.84 MPa, density 2.63 g/cm<sup>3</sup>, open porosity 37.70%, amount of explosive 6.63 kg, powder factor 1.86 kg/m<sup>3</sup> and advance 0.99 m. The number of samples are in parenthesis for each lithotype

$$\xi_i, \xi_i^* \geq 0, i = 1, \dots, l, \varepsilon \geq 0$$

where,  $\mathbf{x}_i \in R^n$  are the inputs,  $y_i \in R^1$  is the target output,  $w$  are the support vectors,  $\phi$  is nonlinear map function,  $C$  is the regularization parameter,  $\xi_i$  and  $\xi_i^*$  are slack variables that represent the distance from the value to the corresponding boundary values of  $\varepsilon$ -tube, and  $l$  is the number of training vectors.

Therefore, the dual problem is

$$\min_{\alpha, \alpha^*} \left\{ \frac{1}{2}(\alpha - \alpha^*)^T \mathbf{K}(\alpha - \alpha^*) + \mathbf{y}^T(\alpha - \alpha^*) \right\} \quad (2)$$

$$\mathbf{e}^T(\boldsymbol{\alpha} - \boldsymbol{\alpha}^*) = 0, \quad \mathbf{e}^T(\boldsymbol{\alpha} + \boldsymbol{\alpha}^*) \leq C\nu$$

$$0 \leq \alpha_i, \quad \alpha_i^* \leq \frac{C}{l}, \quad i = 1, \dots, l$$

where  $\alpha_i$  and  $\alpha_i^*$  are the dual variables and  $\mathbf{K}$  is the Kernel function ( $K = K(x_i, x) = \phi(x_i)^T \phi(x)$ ). Then, the optimal solution is the function

$$f(x) = \sum_{i=1}^l (\alpha_i - \alpha_i^*) \mathbf{K}(x_i, x) + b \quad (3)$$

In the present work, the Kernel selected has been the radial basis function.

$$K_{i,j} = K(\mathbf{x}_i, \mathbf{x}_j) = \exp(-\gamma |\mathbf{x}_i - \mathbf{x}_j|^2) \quad (4)$$

The values of  $C$ ,  $\nu$  and  $\gamma$  are determinate by the Particle Swarm Optimization (PSO) to have regression model that reduces the median absolute percentage error (MdAPE).

### 2.3 Particle Swarm Optimization for the SVR Model

The values of  $C$ ,  $\nu$  and  $\gamma$  for the  $\nu$ -SVR model must be found in such a way that the MdAPE of the SVR model is minimal. This non-linear optimization problem is resolved with computational intelligence-based techniques. In this work, a meta-heuristic algorithm, particle swarm optimization (PSO) [11, 27] is used, based on the social behaviour of the movement of birds flock or swarm of bees [10, 11, 27–30].

Each particle  $i$  of the swarm has a position  $x_i$  defined in the 3-dimensional space ( $C$ ,  $\nu$  and  $\gamma$ ), whose values are a possible solution to minimize the MdAPE of the SVR model. In an iterative way, each particle moves randomly towards the direction where it has found its best personal solution until that moment and in the direction where the best global position  $x_g$  has been found by any of the particles of the swarm. Therefore, all particles explore the region where the best solution has been found. This process follows until the stopping criterion is met.

In our case study, the parameters used to run the PSO are: the number of particles is 100, the ranges of each parameter are  $C \in [0.01, 1000]$ ,  $\nu \in [0.001, 1]$  and  $\gamma \in [0.01, 10]$  and the maximum number of iterations is fixed to 50. Figure 3 shows a flow chart of the PSO-SVR set to obtain the prediction model.

The velocity  $v_i^t$  and position  $x_i^t$  of each particle  $i$  in each iteration  $t$  are updated with the following equations,

$$v_i^t = \omega \cdot v_i^{t-1} + \theta_l \cdot r_l \cdot (x_{il} - x_i^t) + \theta_g \cdot r_g \cdot (x_g - x_i^{t-1}) \quad (5)$$

$$x_i^t = x_i^{t-1} + v_i^t$$

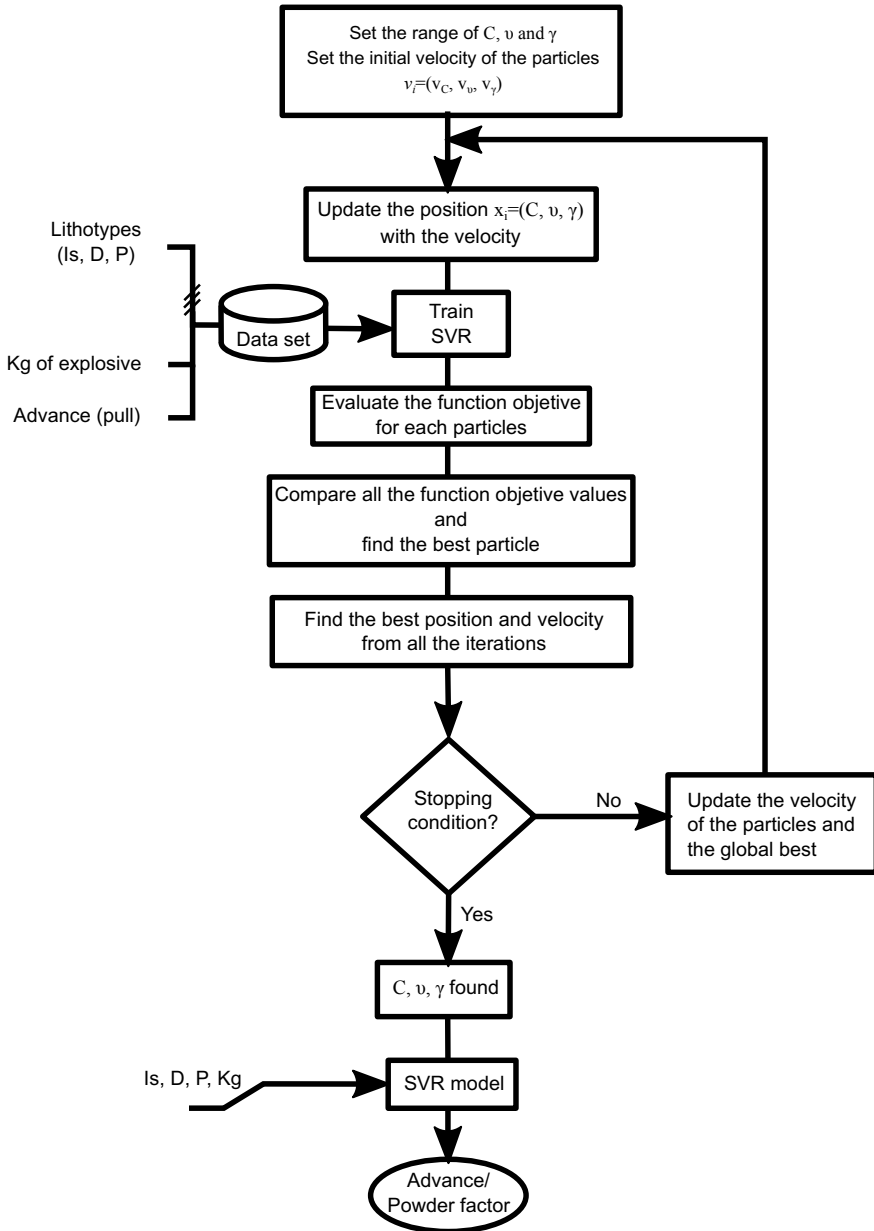


**Fig. 3** Flowchart depicting the algorithm for obtaining the PSO-SVR model. The Flowchart shows the steps used in the Particle Swarm Optimization (PSO) algorithm to determine the  $C$ ,  $v$  and  $\gamma$  values that make the median absolute percentage error (MdAPE) of the SVR model to be minimal (stopping condition)

where  $r_l$  and  $r_g$  are uniform random numbers in the range between 0 and 1,  $\omega$  is the inertial factor  $\omega = 1/|2 - \varphi - \sqrt{\varphi^2 - 4\varphi}|$  with  $\varphi = \varphi_1 + \varphi_2 \geq 4$  [27, 29].  $\theta_l$  is the correction factor to the local best  $\theta_l = \omega\varphi_1$  and  $\theta_g$  is for the global best  $\theta_g = \omega\varphi_2$  with  $\varphi_1 = \varphi_2 = 2.05$ .

The stop condition is that the MdAPE of the global best does not change during  $\Delta k$  iterations. Therefore, “Stop” in iteration  $t = k$  if

$$\sum_{t=k-\Delta k}^k |MdAPE_g^t - MdAPE_g^{t-1}| = 0 \tag{6}$$

with

$$MdAPE_g^t = \min_i \left\{ median \left( \left| \frac{y_{i,j}^t - y_{model,i,j}^t}{y_{i,j}^t} \right|, \forall j = 1, \dots, n_j \right), \forall i = 1, \dots, n_i \right\}$$

where  $n_j$  and  $n_i$  are the number of test samples and the number of particles, respectively. In our case study,  $n_j = 8$ ,  $n_i = 100$  and  $\Delta k = 5$ .

### 2.4 Statistical Analysis

Table 1 shows the average values of point load strength index (Is), open porosity (P), hydrostatic balance density (D), amount of explosive (Ex) and the advance (Ad) for each type of rock. Therefore, if  $X \in \{Is, P, D, Ex, Ad\}$ , the average value of each lithotype is  $E_j(X_{j,i})$  with  $i = 1, \dots, n_j$ , where  $n_j$  is the number of samples for the lithotype  $j$ . The maximum values are  $X_{max} = \max \{E_j(X_{j,i})\}$ . These maximum values,  $\{X_{max}, X \in \{Is, P, D, Ex, Ad\}\}$ , will be used as base values to normalize the training data set,  $x_{j,i}$ , for the PSO-SVR algorithm. The normalized average values from each lithotype,  $\{\bar{x}_j, j \in \{8 \text{ lithotypes}\}\}$ , are used for forecasting the advance, the powder factor and the number of blasts in computer-simulated tunnels where  $x_{j,i} = X_{j,i}/X_{max}$  and  $\bar{x}_j = E_j(X_{j,i})/X_{max}$ .

Figure 4 shows that the probability densities of data do not follow a normal distribution. Therefore, Weibull probability density functions,  $f(X|a, b)$ , were applied with the scale and shape parameters that are showed in Table 2, where

$$f(X|a, b) = \frac{b}{a} \left(\frac{X}{a}\right)^{b-1} \exp \left\{ -\left(\frac{X}{a}\right)^b \right\} \tag{7}$$

$$X \geq 0, \quad a > 0 \text{ (scale)}, \quad b > 0 \text{ (shape)}$$



**Table 1** Characteristic mean parameters for each lithotype. Is, Point load strength index; P, Open porosity; D, Hydrostatic balance density; Ex, Explosive, Ad, Advance

Lithotype (samples)	Is (MPa)	P (%)	D(g/ cm <sup>3</sup> )	Ex (kg)	Ad (m)
Aphanitic massive basalt (5)	3.17	6.70	2.63	5.84	0.91
Altered and highly altered aphanitic massive basalt (5)	0.36	27.39	1.99	5.67	0.97
Vacuolar aphanitic basalt, vacuole <0.05 mm (9)	1.35	24.20	2.09	6.32	0.97
Vacuolar aphanitic basalt, vacuole <0.3 mm (6)	3.82	19.57	2.12	6.63	0.93
Phonolite (4)	5.84	3.78	2.60	6.32	0.86
Red colour ignimbrite (9)	1.06	28.81	1.96	6.49	0.91
Highly altered red colourignimbrite (4)	0.29	35.05	1.82	6.50	0.99
Agglomerate basaltic materials (8)	0.41	37.70	1.65	5.81	0.96
Maximum value	5.84	37.70	2.63	6.63	0.99

## 2.5 Simulation

A simulation application with the new PSO-SVR model and a user-friendly interface (Fig. 5a) (<https://data.mendeley.com/datasets/276fsp2zv2/draft?a=b17cf3bb-70f6-43d8-9772-724ea3c0119b>) has been implemented in GNU Octave [31]. The simulation methodology steps are an adaptation of the method defined by [5] and are:

- 1 Load files with the training data set and the test data set to the PSO-SVR algorithm (steps 1, 2 and 3 in Fig. 5a). The test data set is obtained with the average values calculated for each lithology (Table 1). This test data is used as lithological information to simulate a tunnel (see next steps).
- 2 Run the PSO-SVR algorithm to compute the regression model (step 4). Figure 5b shows an example of the movement evolution of some swarm particles towards solving the optimization problem and the Fig. 5c shows as the MdAPE of the global best solution changes with the number of iterations. When the error does not change in last five iterations means that the solution has been found and the PSO-SVR model is created. Figure 5d shows expected advance for the training and test data set for the best PSO-SVR model.
- 3 Run simulations with the PSO-SVR model. Firstly, a computer-simulated tunnel is defined with information on the distribution of the lithological layers and their thickness. This information is loaded from a file (step 5a in Fig. 5a) and then, after model training, the simulation is ready to run (step 6). The values Is, P, D and Kg of explosive for each lithology are given in the test data set loaded in the step 2. In the area between two different lithotypes, the characteristics Is, P, D and Kg of explosive are taken according to the proportion in which they are found in the simulated drill. Finally, the simulation runs and the final results

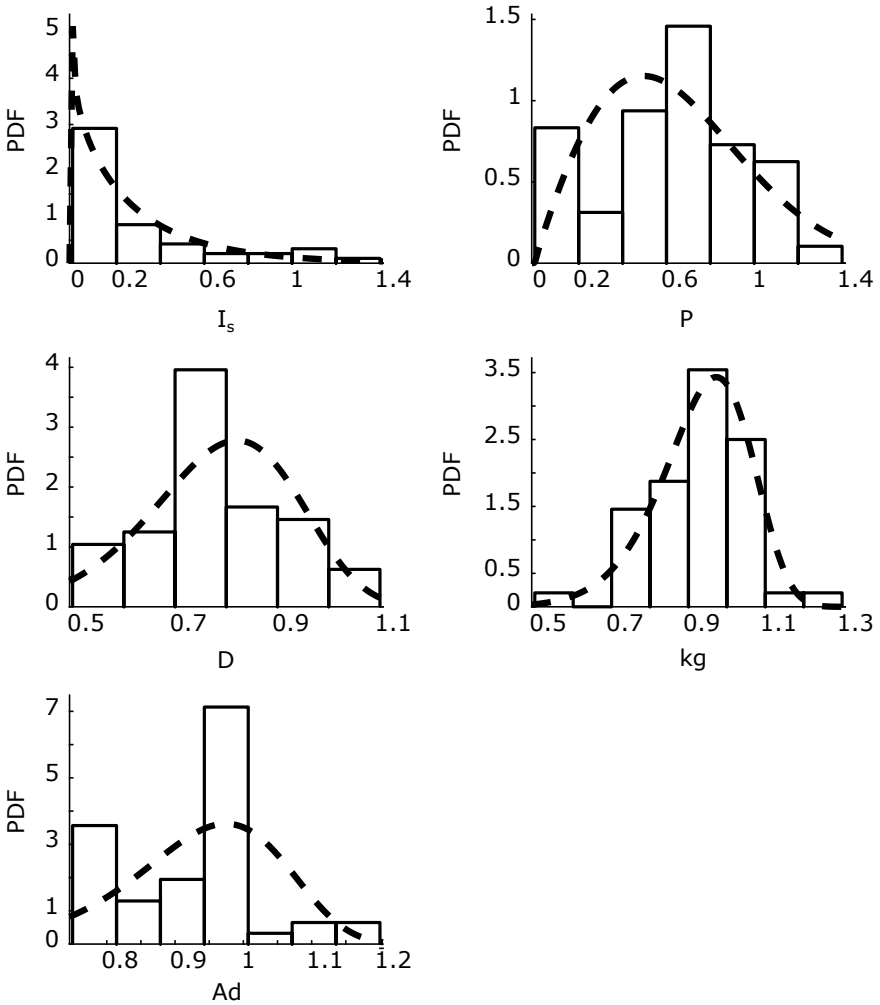


**Fig. 4** The probability density functions (PDF) for the normalized data set used to train the PSO-SVR. The PDFs are adjusted with Weibull functions, which parameters are in Table 2

**Table 2** Characteristic mean parameters for each lithotype

Parameters	a (scale)	b (shape)
Point load strength index ( $I_s$ )	0.2924	0.9259
Open porosity ( $P$ )	0.7250	1.9181
Hydrostatic balance density ( $D$ )	0.8438	6.2883
Explosive	0.9847	9.1331
Advance	0.9857	9.6412

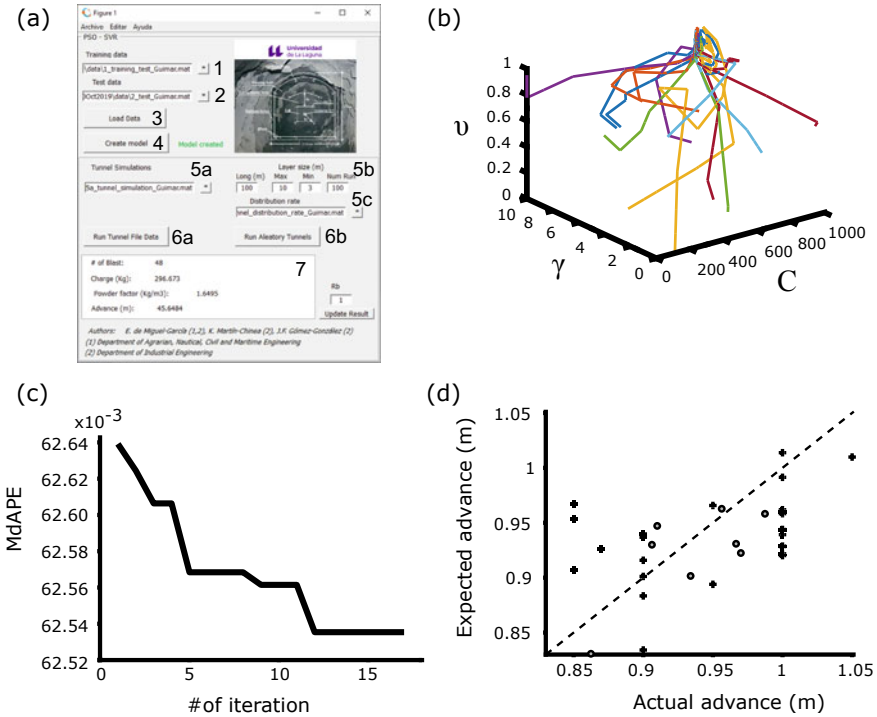


**Fig. 5** PSO-SVR algorithm training and testing. **a** User interface of Octave application developed to compute the PSO-SVR model and to run the Simulations. The numbers one to seven indicate the steps to follow to create the model, to run the model and to display results. See the text to have more information. **b** Movement of some particles of the PSO algorithm in the space  $(C, \gamma, \nu)$  toward the solution. **c** The median absolute percentage error (MdAPE) of the SVR model decreases with the number of iteration of the PSO algorithm. **d** Expected advances versus actual advances are plotted for the training data (crosses) and the test data set (dots) using the PSO-SVR model

(number of blast, the amount of explosive (kg), the advance (m) and the powder factor ( $\text{kg}/\text{m}^3$ )) are displayed on a panel (step 7).

If the lithological distribution of a tunnel is unknown, a probable solution will be calculated using a set of computer-simulated tunnels. In this case, the needed parameters to build the computer-simulated tunnels are the length of the tunnel, the maximum and the minimum layer sizes and number of tunnels to do the statistical study (step 5b). The characteristics  $I_s$ ,  $P$ ,  $D$  and  $K_g$  of explosive for each lithology is taken from the test data set (step 2) and the percentage of the distribution expected to be found of each lithology defined in the test data, has to be loaded from a file (step 5c). In our study case, the percentage of each lithology is given in Table 3. After providing these parameters, the calculation can be executed (step 6b) and the results will be displayed on the panel (step 7). These results are computed as the average of the individual results of all tunnels. Figure 6a shows three examples of computer-

**Table 3** Real lithotype distribution of the Güimar tunnel for the simulation using a computer-designed tunnel

Lithotype	Total length (m)	Probability (%)
Aphanitic massive basalt	4.55	10
Altered and highly altered aphanitic massive basalt	4.85	11
Vacuolar aphanitic basalt vacuole <0.05 mm	8.70	19
Vacuolar aphanitic basalt, vacuole <0.3 mm	4.67	10
Phonolite	3.45	8
Red colour ignimbrite	7.25	16
Highly altered red colour ignimbrite	3.95	9
Agglomerate basaltic materials	7.65	17

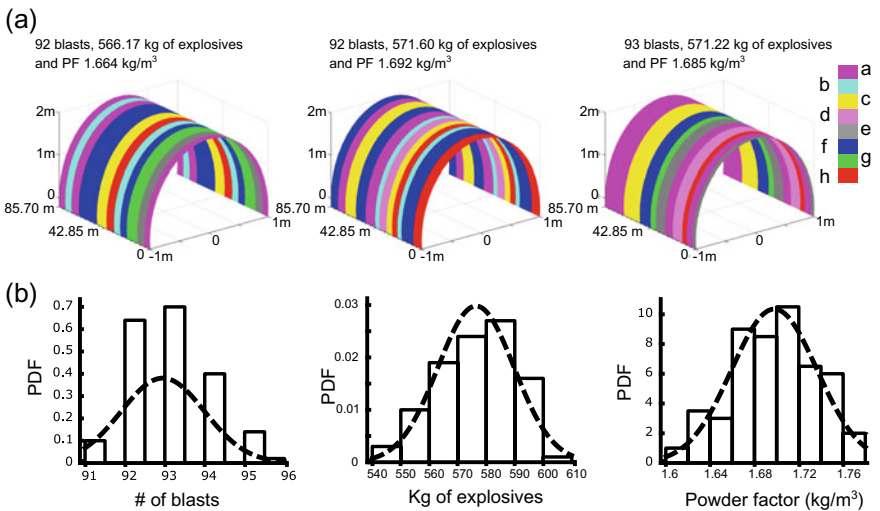


**Fig. 6** Computer-simulated tunnels. **a** Three examples of computer-simulated tunnels with different lithologies used to computed the most probable value for the number of blasts, the quantity of explosives and the powder factor for a tunnel of 85.70 m. The colour bar for lithotypes: (a) aphanitic massive basalt, (b) altered and highly altered aphanitic massive basalt, (c) vacuolar aphanitic basalt, vacuole <0.05 mm, (d) vacuolar aphanitic basalt, vacuole <0.3 mm, (e), phonolite, (f) red colour ignimbrite, (g) highly altered red colour ignimbrite and (h) agglomerate basaltic materials. **b** The probability density functions (PDF) and the Gaussian adjustments of the number of blasts, the quantity of explosives and the powder factor calculated using 100 tunnels

simulated tunnels and the probability density function for the amount of explosive (kg), number of blasts and the powder factor (kg/m³) calculated using 100 tunnels.

Simulations and data analysis were performed using the application of Excel spreadsheets (Microsoft® Office), GNU Octave [31] and MATLAB® (Mathworks Inc., Natick, MS, USA). The SVM model is implemented with the library LIBSVM [26].

### 3 Results and Discussion

#### 3.1 Relationship Between Lithotypes and Powder Factor

A representative image of the eight lithotypes extracted from the stretch of 85.70 m, at a distance of 4000 m from the entrance of the tunnel, are showed in Fig. 2a. The lithotypes with their geomechanical features (point load strength index  $I_s$  (MPa), open porosity  $P$  (%) and hydrostatic balance density  $D$  ( $\text{g}/\text{cm}^3$ )) are shown in Fig. 2a where the values correspond to the mean values normalized by maximum averaged value.

Figure 2b shows the normalized mean explosive charge used, the normalized mean advance and the normalized mean powder factor (relationship between how much explosive (kg) and volume of rock broken ( $\text{m}^3$ )) for each lithotype. The normalizations were done by the maximum averaged values (to see Table 1).

Data show that the relationship between the powder factor and the geomechanical features of each lithotype is not straightforward. In fact, Fig. 2 shows that highly altered red colour ignimbrite has a lower  $I_s$ , a lower  $D$  and a higher  $P$  than phonolite, but their powder factors are similar. Another example is the case of altered and highly altered aphanitic massive basalt and red colour ignimbrite that have similar  $P$  and  $D$ , however, they have a different powder factor. Therefore, non-linear relationships between statistical values between the characteristics of the lithotypes and the powder factor should be sought as it was done by [5].

In this work, it is proposed that methods used in Machine Learning and Data Science, such as SVR and PSO, could be successful in finding a regression model that provides the powder factor if the geomechanical characteristics of the rock and the usual explosive charge applied by technicians and/or engineers are known.

#### 3.2 Forecasting of the Advance and the Powder Factor with a PSO-SVR Model

In our case study, to 85.70 m in a real underground water volcanic tunnel, not only blasts were used, but also excavations by an overshot mucker and pneumatic breakers, since they did not need explosives. Therefore, a percentage of length perforated by explosives,  $R_b$ , is defined. In our case, this value is  $R_b = 52.59\%$ , 45.07 m pulled with explosives of the 85.70 m driven.

Experimentally, 48 blasts 297.25 kg of explosive with a powder factor of 1.67  $\text{kg}/\text{m}^3$  were needed to 45.07 m using a drill of 1.2 m. Theoretically, the commonly used formula defined by Langefors and Kihlstrom (Langefors and Kihlstrom, 1973) applied to the design of small tunnel drilling, forecasts 40 blasts assuming that the advance is 95% of the drilling length (1.2 m). Where the traditional formulation assumes a constant of the rock 'c' of 0.4 and estimates that the advance is 1.14 m per pull. Hence, the difference between the actual and the predicted values could be

due to the specific geomechanical characteristics of the rock that are not taken into account in each blast. When a tunnel designed by computer with the same type, order and length of rock slices presented in the Table 3 and taken account the characteristics of Is, P, D and Ex given in Table 1, is applied to the PSO-SVR model the results are: 49 blasts, 302.58 kg of explosive with a powder factor of 1.69 kg/m<sup>3</sup>. Therefore, the number of blasts predicted by the PSO-SVR model is significantly close to that obtained in the real civil work. In addition, the amount of explosives and the powder factor predicted by the model are very close to the real ones.

If the study is carried out for a single type of rock (Tables 4 and 5), the estimated actual advances and powder factors for different lithologies can be compared with those predicted by the PSO-SVR model and the formulation of Langefors and Kihlstrom (L-K). In all the cases, the results show that the PSO-SVR model gives the best estimations with a relative deviation of the estimated that goes between 0.57% and 7.91%, however the L-K goes between 12.29% and 23.47%.

The probability of distribution of the different lithologies in a tunnel (see Table 3 case of Güimar tunnel) can be estimated with the rock samples taken. Hence, the amount of explosives and the powder factor needed to drive a tunnel can be predicted using the lithological distribution, the PSO-SVR model and the percentage of driving expected by explosives. Because the order in which the different layers are distributed and their thicknesses are unknown, multiple computer-simulated tunnels are made to obtain statistically significant values. Where each tunnel is constructed with randomly arranged layers following the probabilistic distribution of the experimentally obtained lithology (Table 3) with randomly chosen thicknesses (for example, between 3 and 10 m in our study case). Table 6 shows the results obtained using 100, 1000 and 10,000 simulations for 85.70 m tunnel. These results are similar to the experimental

**Table 4** Comparison of the actual estimated advances for different lithologies with the predicted advances by PSO-SVR model and the formulation of Langefors and Kihlstrom. The average values for the advance are shown for each blast as function of the lithology and amount of explosive per blast used in the study case to drive the tunnel. Ex, Explosive; Ad, Advance; PSO-SVR, Hybrid model based on Particle Swarm Optimization and Support Vector Regression; L&K, forecast based on the formulation of Langefors and Kihlstrom

Lithology	Actual		PSO-SVR	L&K
	Ex (kg)	Ad (m)	Ad (m)	Ad (m)
Aphanitic massive basalt	5.84	0.91	0.95	1.14
Altered and highly altered aphanitic massive basalt	5.67	0.97	0.92	1.14
Vacuolar aphanitic basalt, vacuole <0.05 mm	6.32	0.97	0.93	1.14
Vacuolar aphanitic basalt, vacuole <0.3 mm	6.63	0.93	0.90	1.14
Phonolite	6.33	0.86	0.83	1.14
Red colour ignimbrite	6.49	0.91	0.93	1.14
Highly altered red colour ignimbrite	6.50	0.99	0.96	1.14
Agglomerate basaltic materials	5.81	0.96	0.96	1.14

**Table 5** Comparison of the actual estimated powder factors for different lithologies with the predicted powder factors by PSO-SVR model and the formulation of Langefors and Kihlstrom. The average values for the powder factor are shown for each blast as function of the lithology and amount of explosive per blast used in the study case to drive the tunnel. PF, powder factor; PFDev, relative deviation of the estimated PF versus the experimental PF; PSO-SVR, Hybrid model based on Particle Swarm Optimization and Support Vector Regression; L&K, forecast based on the formulation of Langefors and Kihlstrom

Lithology	Actual	PSO-SVR		L&K	
	PF (kg/m <sup>3</sup> )	PF (kg/m <sup>3</sup> )	PFDev (%)	PF (kg/m <sup>3</sup> )	PFDev (%)
Aphanitic massive basalt	1.63	1.57	3.96	1.30	20.23
Altered and highly altered aphanitic massive basalt	1.48	1.56	5.43	1.26	14.71
Vacuolar aphanitic basalt, vacuole <0.05 mm	1.66	1.72	3.87	1.41	15.21
Vacuolar aphanitic basalt, vacuole <0.3 mm	1.73	1.87	7.91	1.48	14.68
Phonolite	1.84	1.93	5.03	1.41	23.47
Red colour ignimbrite	1.74	1.77	1.77	1.44	16.99
Highly altered red colour ignimbrite	1.65	1.72	4.35	1.45	12.29
Agglomerate basaltic materials	1.54	1.53	0.57	1.29	16.06

**Table 6** Computation of the number of blasts and the powder factor using a computer-simulated tunnel with a lithological distribution based on that found in a real tunnel and the PSO-SVR model estimated with raw data set. Long, length of the tunnel to drive; Ex, Explosive; PF, powder factor; Rb is the percentage of tunnel to drive using explosive. For the simulation the type of lithology, arrangement and lengths of the rock slice are chosen randomly following the probabilistic distribution found in the Güimar tunnel. The slice length is between 3 and 10 m

# of runs	Long (m)	Rb (%)	# of blasts	Ex (kg)	PF (kg/m <sup>3</sup> )
100	85.70	52.59	49	301.5	1.69
1000	85.70	52.59	49	303.17	1.70
10000	85.70	52.59	49	303.2	1.70
Real data	85.70	52.59	48	297.25	1.65

ones and there are no differences between the numbers of simulations used. Figure 6b shows the results obtaining for a simulation with 100 tunnels 85.70 m where the probability density function (PDF) of the number of blasts, kilograms of explosives and the powder factor have a Gaussian probability density functions. Therefore, from this Gaussian PDF is able to obtain the more probable prediction of number for blasts (93) and total of kilograms of explosives (576.4 kg) needed to drive the tunnel.

**Table 7** Computation of the number of blasts and the powder factor using a computer-simulated tunnel with a lithological distribution based on that found in a real tunnel and the PSO-SVR model estimated with average data set (Table 1). Long, length of the tunnel to drive; Ex, Explosive; PF, powder factor; Rb is the percentage of tunnel to drive using explosive. For the simulation the type of lithology, arrangement and lengths of the rock slice are chosen randomly following the probabilistic distribution found in the Güimar tunnel. The slice length is between 3 and 10 m

# of runs	Long (m)	Rb (%)	# of blasts	Ex (kg)	PF (kg/m <sup>3</sup> )
100	85.70	52.59	48	295.19	1.65
1000	85.70	52.59	48	296.04	1.66
10000	85.70	52.59	48	296.09	1.66
Real data	85.70	52.59	48	297.25	1.65

### 3.3 PSO-SVR Model Trained with a Small Average Data Set

In a new civil work where a survey cannot be carried out to obtain information on the lithological distribution, a PSO-SVR model could be obtained if the following information is available: the average values of the geomechanical characteristics of the existing lithologies in the area, the probability to find each type of lithology (obtained by geological studies of the area, probes or nearby tunnels) and the amount of explosives that is generally used in each explosion depending on the type of rock. In this case, although, the number of data is small, it is possible to obtain a PSO-SVR regression model to make predictions. To verify that a PSO-SVR model can be obtained, we suppose that the training data set is the average values *I*, *P*, *D*, *Ex* and *Probability* given in Tables 1 and 3. Table 7 shows predictions for computer-designed tunnels build randomly using the PSO-SVR model and the computed results using the average data set reproduce significantly the experimental ones.

## 4 Conclusion

Engineers must design civil work projects for the construction of new tunnels or increase the length of existing ones, as in our case study. In these civil engineering projects, the duration of civil works, the number of blasts, the amount of explosives required, etc. should be evaluated to better estimate the necessary project budget.

Until now, the formulation of Langefors and Kihlstrom had been one of the best known methods to estimate the advance and the powder factor. However, as the results showed, their predictions were far from the actual data that had been obtained in our case study. The need for a better estimate of the 'c' parameter greatly influences this prediction. In the present study, it has been shown that a SVR-based model can give a good prediction of the advance and the powder factor without the need to develop a complex formulation. To set the parameters of the SVR, a PSO algorithm was applied. Therefore, this study proposes a new tool (a hybrid PSO-SVR model) that



will help engineers develop their projects giving predictions closer to reality about the amount of explosives, the number of blasts needed and the duration of the civil works.

**Acknowledgements** The authors would like to thank the owners of the La Paloma water tunnel and the Service of Laboratories and Quality of Construction of the Ministry of Public Works and Transport, Vice-Ministry of Infrastructure and Transport of the Government of the Canary Islands, Spain for their collaboration in this research work.

**Conflict of Interest Statement.** None declared.

## References

1. Nasiri F, Mafakheri MS (2015) Qanat water supply systems: a revisit of sustainability perspectives. *Environ Syst Res* 4(13):1–5
2. Langefors U, Kihlstrom B (1973) *The modern technique of rock blasting*, 2nd edn. Wiley, New York. <https://trove.nla.gov.au/work/10826003>
3. Persson PA, Holmberg R, Lee J (1993) *Rock and explosives engineering*. CRC Press, New York
4. Holmberg R (1982) Charge calculations for tunneling. In: Hustrulid WA (ed) *Underground mining methods handbook*, SME, pp 1580–1589. U.S. Department of Energy Office of Scientific and Technical Information
5. de Miguel-García E, Gómez-González J (2019) A new methodology to estimate the powder factor of explosives considering the different lithologies of volcanic lands: a case study from the island of Tenerife, Spain. *Tunnell Underground Space Technol* 91:103023. <https://www.sciencedirect.com/science/article/pii/S088677981830659X?via%3Dihub>
6. Smola AJ, Schölkopf B (2004) A tutorial on support vector regression. In: *Statistics and computing*. Kluwer Academic Publishers, pp 199–222
7. Vapnik V, Golowich SE (1996) Support vector method for function approximation, regression estimation, and signal processing. *Advances in neural information processing systems*, pp 281–287 (1996)
8. Vapnik VN (1995) *The nature of statistical learning theory*. Springer New York. <http://link.springer.com/10.1007/978-1-4757-2440-0>
9. Boser BE, Guyon IM, Vapnik VN (1992) A training algorithm for optimal margin classifiers. In: *Proceedings of the annual conference on computational learning theory*, pp 144–152. ACM Press, Pittsburgh, PA. <http://www.svms.org/training/BOGV92.pdf>
10. Gaing ZL (2004) A particle swarm optimization approach for optimum design of PID controller in AVR system. *IEEE Trans Energy Convers*
11. Eberhart R, Kennedy J (1995) A new optimizer using particle swarm theory. In: *Sixth international symposium on micro machine and human science*. IEEE, New York, pp 39–43
12. Li Q, Fu Y, Zhou X, Xu Y (2010) A hybrid support vector regression for time series prediction. In: *3rd international conference on knowledge discovery and data mining, WKDD 2010*, pp 506–509 (2010)
13. Liu S, Tai H, Ding Q, Li D, Xu L, Wei Y (2013) A hybrid approach of support vector regression with genetic algorithm optimization for aquaculture water quality prediction. *Math Comput Modell* 58:458–465
14. Kaneda Y, Mineno H (2016) Sliding window-based support vector regression for predicting micrometeorological data. *Expert Syst Appl*
15. Shamshirband S, Petkovic D, Javidnia H, Gani A (2015) Sensor data fusion by support vector regression methodology - A comparative study. *IEEE Sens J* 15:850–854
16. Trafalis T, Ince H (2000) Support vector machine for regression and applications to financial forecasting. *IEEE, New York*, pp 348–353

17. Zukas JA, Walters WP (1998) Explosive effects and applications. Springer, New York
18. International Society of Explosives Engineers (1998) The Blasters' Handbook. ISEE, Cleveland, USA
19. Lopez Jimeno C, Lopez Jimeno E, Ayala Carcedo FJ, Visser de Ramiro Y (2017) Drilling and blasting of rocks. Taylor & Francis, London. <http://www.worldcat.org/title/drilling-and-blasting-of-rocks/oclc/1020789548>
20. Jimeno CL, Bermúdez PG (2003) Avances tecnológicos en el campo de la perforación y voladura de rocas. Ingeopress, p 7
21. Fúster JM, Páez A, Sagredo J (1969) Significance of basic and ultramafic rock inclusions in the basalts of Canary Islands. *Bulletin Volcanologique* 33(3):665–693
22. Cortes C, Vapnik V (1995) Support-vector networks. *Mach Learn* 20:273–297
23. Chang CC, Lin CJ (2002) Training v-support vector regression: theory and algorithms. *Neural Comput* 14(8):1959–1977
24. Tan M, Song X, Yang X, Wu Q (2015) Support-vector-regression machine technology for total organic carbon content prediction from wireline logs in organic shale: a comparative study. *J Nat Gas Sci Eng* 26:792–802
25. Schölkopf B, Bartlett P, Smola A, Williamson R, First GMD, Chaussee R (1999) Shrinking the tube: a new support vector regression algorithm. In: *Advances in neural information processing systems*, pp 330–336
26. Chih-Chung C, Chih-Jen L (2011) LIBSVM : a library for support vector machines. *ACM Trans Intell Syst Technol* 2:1–27. <http://www.csie.ntu.edu.tw/~cjlin/libsvm>
27. Clerc M, Kennedy J (2002) The particle swarm-explosion, stability, and convergence in a multidimensional complex space. *IEEE Trans Evol Comput* 6(1):58–73
28. van den Bergh F, Engelbrecht AP (2004) A cooperative approach to particle swarm optimization. *IEEE Trans Evol Comput* 8(3):225–239
29. del Valle Y, Venayagamoorthy GK, Mohagheghi S, Hernandez JC, Harley RG (2008) Particle swarm optimization: basic concepts, variants and applications in power systems
30. Varthanan PA, Murugan N, Kumar GM (2012) A simulation based heuristic discrete particle swarm algorithm for generating integrated production-distribution plan. *Appl Soft Comput J* 12:3034–3050
31. Eaton JW, Bateman D, Hauberg S, Rik W (2019) GNU Octave version 5.1.0 manual: a high-level interactive language for numerical computations. <https://www.gnu.org/software/octave/doc/v5.1.0/>